Available online at www.sciencedirect.com
ScienceDirect
Journal of Controlled Release 124 (2007) 134–143
journal of controlled release
www.elsevier.com/locate/jconrel

Transport mechanisms of mmePEG$_{750}$P(CL-co-TMC) polymeric micelles across the intestinal barrier

Frédéric Mathot [a], A. des Rieux [a,b], A. Ariën [c], Y-J. Schneider [b], M. Brewster [c], V. Préat [a,*]

[a] Université catholique de Louvain, Unité de Pharmacie Galénique, Avenue E. Mounier 73.20, U.C.L., 1200 Brussels, Belgium
[b] Université catholique de Louvain, Institut des Sciences de la Vie, Laboratoire de Biochimie cellulaire, Croix du Sud 5, U.C.L., 1348 Louvain-la-Neuve, Belgium
[c] Johnson & Johnson, Pharmaceutical Research and Development, Division of Janssen Pharmaceutica, 2340 Beerse, Belgium

Received 6 July 2007; accepted 3 September 2007
Available online 7 September 2007

Abstract

Monomethylether poly(ethyleneglycol)$_{750}$-poly(caprolactone-co-trimethylene carbonate) (mmePEG$_{750}$P(CL-co-TMC)) which spontaneously form micelles, can cross lipid bilayers via passive diffusion and demonstrate an oral bioavailability of 40% in rats. The aim of the current work was to study the transport mechanism(s) of drug-loaded mmePEG$_{750}$P(CL-co-TMC) micelles across the intestinal barrier. The transport of radiolabelled polymer across Caco-2 cell monolayer was investigated by disrupting tight junctions and by inhibiting endocytosis. The polymer and drugs loaded in micelles independently crossed Caco-2 cell monolayers and did not use either the paracellular route or M-cells. The polymer did not affect P-gp pumps. This mechanistic study suggests that whereas drug-loaded micelles were absorbed by fluid-phase endocytosis, polymeric unimers diffused passively across the membrane concomitantly with micellar endocytosis.

Keywords: Self-assembling polymeric micelles; mmePEG$_{750}$P(CL-co-TMC); Caco-2; FAE model; Endocytosis, Passive diffusion

1. Introduction

The ability to formulate contemporary pharmaceutical drug candidates is becoming more and more difficult. This is due to the ever increasing challenges presented as a function of physical chemical properties of small molecules therapeutics which over the years have tended to become more lipophilic, of lower water-solubility, of higher molecular weight. Polymeric micelles are therefore increasingly attractive as modalities to address issues on the solubilization of poorly water-soluble drugs. They entrap drug inside the core associated with the lipophilic moiety of the amphiphilic surfactant; the hydrophilic part forming the outer shell of this nanocarrier [1–5]. In addition to solubilization, the active pharmaceutical ingredient (API) so encapsulated can be protected from degradation caused by the aqueous environment. These polymeric micelles, which result from the assembling of polymeric unimers above their critical micellar concentration, therefore represent a technological advantage as they provide a greater capacity for drug solubilization as well as a higher stability in physiological media compared with classic surfactant-forming micelles.

Since the majority of polymeric micelles is intended to be administered intravenously [6–9], a new class of micelles has been developed in order to deliver them most effectively via the oral route [10–12]. The polymeric material mmePEG$_{750}$P(CL-co-TMC) [monomethylether poly(ethylene glycol)$_{750}$-poly(caprolactone-co-trimethylene carbonate)] is an example of this new category of amphiphilic polymer which is able to self-assemble and entrap drug. Preconcentrates are prepared by simply mixing the drug and liquid polymer avoiding the complex preparation associated with other approaches. The preconcentrate spontaneously forms the micelles upon contact with gastric media. [13–15]. We previously demonstrated that mmePEG$_{750}$P(CL-co-TMC) crosses enterocyte monolayer of Caco-2 cells and has an oral bioavailability of 40% in rats, allowing a sustained plasma profile of the co-administered drug [15].

The mechanism by which polymeric surfactants and micelles formed therefrom cross the intestinal barrier remains uncertain.

* Corresponding author. Tel.: +32 2 764 73 20; fax: +32 2 764 73 98.
E-mail address: veronique.preat@uclouvain.be (V. Préat).

0168-3659/$ - see front matter © 2007 Elsevier B.V. All rights reserved.
doi:10.1016/j.jconrel.2007.09.001

Several studies have suggested that endocytosis, occurring most probably by fluid-phase pinocytosis, could explain the transport of polymeric micelles across biological membranes [16–18], although definitive proof is still lacking. Recently, we provided evidence of passive diffusion of mmePEG$_{750}$P(CL-co-TMC) polymer (most likely unimers in equilibrium with micelles) across an enterocyte-mimicking bilayer (PAMPA system) at a concentration that did not perturb the membrane integrity [19]. To better characterize transport mechanism(s) through the intestinal barrier, we investigated various alternative paths that could be taken by the mmePEG$_{750}$P(CL-co-TMC) in the passage across enterocytes. The paracellular route as well as the endocytic pathways were therefore explored, keeping in mind that passive diffusion was already demonstrated. In addition, based on the observation that certain polymeric surfactants, in particular some of the Pluronics, can inhibit the P-gp molecular pump [20,21], we checked the potentially inhibitory effect of mmePEG$_{750}$P(CL-co-TMC) on this pump which is present at the apical side of enterocytes. Two different cell models representing intestinal cell lines were used in this study: Caco-2 cell monolayers (human colorectal carcinoma cells) mimicking human enterocytes and a model of the human follicle-associated epithelium (FAE). The FAE model consists in a co-culture system of Caco-2 cells and human Raji B lymphocytes mimicking the FAE population which is mainly composed of M-cells and enterocytes. The FAE is a particular structure found in Peyer's patches in which M-cells play a special role due to their increased endocytosis activity. This model was used for its well-recognized ability to transport a wide range of materials, including macromolecules via transcytosis [22–24].

2. Materials and methods

2.1. Synthesis and characterization of polymers

Copolymer (mmePEG$_{750}$P(CL-co-TMC) was synthesised by the Johnson & Johnson Center for Biomaterials and Advanced Technologies (CBAT, Somerville, NJ, USA). Monomethylether-polyetheleneglycol with a molecular weight of 750g/mol (mmePEG$_{750}$) was purchased from Fluka (Milwaukee, WI, USA). ε-caprolactone (CL) was obtained from Union Carbide (Danbury, CT, USA), and trimethylene carbonate (TMC) from Boehringer Ingelheim (Petersburg, VA, USA). Stannous octoate and toluene were obtained from Aldrich (Milwaukee, WI, USA). The radiolabelled [^{14}C]-mmePEG$_{750}$P(CL-co-TMC) (50:50 molar ratio) polymer was synthesised by Perkin-Elmer.

Ring opening polymerization was carried out to prepare the mmePEG$_{750}$P(CL-co-TMC) diblock polymers as described earlier [14, 25, 26]. Radiolabelling of mmePEG$_{750}$P(CL-co-TMC) was generated by replacing unlabelled ε-caprolactone by ε-[caprolactone-2,6-^{14}C] during the polymerization.

The polymer composition and residual monomer content were analysed by proton NMR. Gel permeation chromatography was utilized to determine the weight-average molecular weight and the polydispersity of the polymers [13,14]. The radiochemical purity of [^{14}C]-mmePEG$_{750}$P(CL-co-TMC) was assessed using a HPLC system equipped with a radioactivity detector [15].

2.2. Characterization of micelle physicochemical properties

Micelle size was determined by dynamic light scattering (DLS) and zeta potential was measured by laser Doppler velocimetry combined with phase analysis light scattering (PALS), both using a Zetasizer® Nano ZS (Malvern Instruments, UK). Measurements were performed in citrate-citric acid buffer pH 6.0 (300mOsm/kg). Their size and ζ potential were found to be 24.15nm (PDI: 0.052) and − 2.7mV (width: 13.2), respectively. The size of the micelles was not influenced by the concentration of the polymer. The polymer critical micellar concentration (CMC) was measured by fluorimetry (as described previously [13,14]) and was in the range of 20μg/ml (0.002%; w/v). The chemical composition of the polymers as determined by proton NMR was in good agreement with the ratio of the charged monomers with the CL/TMC molar ratio for mmePEG$_{750}$P (CL-co-TMC) being 49/49 mole/mole. The residual monomer content was less than 1mol%. The weight-averaged molecular weight (Mw) of mmePEG$_{750}$P(CL-co-TMC) and [^{14}C]-mmePEG$_{750}$P(CL-co-TMC) were 5242Da (PD = 1.9) and 5188Da (PD = 1.6), respectively. The [^{14}C]-mmePEG$_{750}$P (CL-co-TMC) polymer had a radiochemical purity of ≥ 97% with a specific activity of 1.13μCi/mg. The polymers were liquid at room temperature and formed micelles spontaneously on contact with aqueous media.

2.3. In vitro cell models used to study transport mechanisms

2.3.1. Cell cultures

Caco-2 cells were routinely maintained in plastic culture flasks (162cm^2) (Corning Incorporated, NY, USA) with 0.2-μm vent cap. The cells were obtained from the American Type Culture Collection (ATCC), and were used between passage 76 and 85. The cultures were mycoplasma free (mycoplasma detection kit; Roche GmbH, Mannheim, DE). The cells were subcultivated before reaching confluence. Caco-2 cells were harvested with 0.25% (w/v) trypsin and 0.2% (w/v) EDTA (5–15min) at 37°C and seeded in new flasks. The culture medium, Dulbecco's Modified Eagle Medium (DMEM), was supplemented with 1% non-essential amino acids (NEAA), 2mM L-glutamine, 100U/ml penicillin/streptomycin and 10% fetal bovine serum (FBS). Caco-2 monolayers were obtained by seeding 1.5 × 10^5 cells/cm^2 on Transwell polycarbonate inserts (12mm insert diameter, 0.4μm pore size) (Corning Costar, Cambridge, U.K.) and culturing them for 21days. The culture medium was replaced every other day. All supplements and cell culture media were purchased from Invitrogen (Merelbeke, BE).

The inverted human follicle-associated epithelium model (FAE) was obtained by co-culturing monoclonal Caco-2 cells (clone 1) with human Raji cells as described by des Rieux et al. [22,23]. Briefly, 3 to 5days after Caco-2 cells clone 1 seeding, the inserts were inverted and a piece of silicon tube was slipped onto the basolateral side of each insert. The inverted inserts were maintained for the next 9–11days in large Petri dishes. Raji cells (human Burkitt's lymphoma Raji B line from ATCC) were then added to the basolateral compartment and the co-cultures were maintained inverted for 5days until the transport experiment.

2.3.2. Assessment of cell monolayer integrity

Measurements of trans-epithelial electrical resistance (TEER) were used to determine the integrity of the cell monolayers. Monolayer TEER's were measured at 37°C using an Evom resistance volt-ohm meter (World Precision Instruments, Berlin, DE). Caco-2 cell and FAE monolayers presenting with TEER values below 400Ω cm^2 and 150Ω cm^2, respectively, were excluded from the experiments. The resistance of HBSS alone (9Ω cm^2) was considered as background resistance and subtracted from each TEER value. TEER values were compared before and after the transport studies [15]. Unless stated otherwise, TEER values after transport studies were not significantly different of initial values.

Toxicity of different treatments applied to cell monolayers was assessed by measuring the lactate dehydrogenase (LDH) activity released from the cytosol of damaged cells (Roche Diagnostics Belgium, Vilvoorde, BE). The LDH release induced by the mmePEG$_{750}$P(CL-co-TMC) alone did not exceed 1%, even for the highest polymer concentration (3%).

2.4. Transport mechanisms of unimers and drug-loaded polymeric micelles

2.4.1. Drug-loaded micelle formulations

Appropriate amounts of radiolabelled and unlabelled mmePEG$_{750}$P(CL-co-TMC) at concentrations above 0.1% (w/v) were mixed for 1h in Hanks' balanced salt solution (HBSS) to form micelles [15]. When model drugs of sparingly soluble pharmaceuticals (carbamazepine and chlorothiazide) (Sigma, Bornem, BE) were used, they were always solubilized to saturation in the mmePEG$_{750}$P(CL-co-TMC) systems. To this end, an excess of drug was mixed overnight with the polymer. The unsolubilized drug fraction was removed by filtration through a 0.45-μm PVDF Chromafil® filter (Düren, DE) after adding the buffer. The two key parameters that guided the choice for these model drugs were that they exclusive permeate the intestinal barrier via passive diffusion [27,28] and that they are not reported to be substrate for efflux pumps [29]; rather than the solubility improvement provided by the mmePEG$_{750}$P(CL-co-TMC). Polymer and drug concentrations were subsequently checked by liquid scintillation and HPLC-UV, respectively.

2.4.2. Transport experiments

For all transport studies, the Caco-2 cell monolayers were washed twice with HBSS (0.5ml in the apical compartment and 1.5ml in the basolateral side) for 30min at 37°C. In order to investigate the apical to basolateral transport (A to B), 500μl of the formulations of interest were added at the apical side of inserts while the basolateral compartments were filled with HBSS. For the basolateral to apical transport (B to A), 1.5ml of the formulations was added at the basolateral side while the apical compartments were filled with HBSS. The amount of polymer crossing the cell monolayers was assayed by sampling 400μl of buffer from the receiver compartments after 120min of incubation at 37°C (unless stated otherwise). To verify if the passage kinetics of carbamazepine and chlorothiazide loaded or not in 3% mmePEG$_{750}$P(CL-co-TMC) was linear, sampling of receiver compartments was realized every 30min for 120min and the amount of polymer and drug (carbamazepine or chlorothiazide) crossing the monolayer was assayed by removing 1.5ml of buffer from the basolateral compartments after 30, 60, 90 and 120min. Radioactive samples were placed in 4ml of scintillation cocktail (Aqualuma, Lumac, Groningen, NL) and were analyzed using a Wallac 1410 Liquid Scintillation Counter (Pharmacia) with automatic external standardization. Samples containing chlorothiazide or carbamazepine were analyzed by HPLC-UV using published assays [30,31], which were modified to render them compatible with our laboratory conditions. In both cases, analyses were performed on an Agilent 1100 series (Agilent Technologies, Diegem, BE) HPLC equipped with a quaternary pump, a vacuum degasser and a UV–vis detector. The thermostatted column (Hypersil BDS C18, 3μm, 100 × 4.6mm protected by a guard column Hypersil ODS, 5μm, 4.0 × 20mm (Alltech, Lokeren, BE)) was set at 30°C. Standard curves for chlorothiazide were prepared in the concentration range of 1.0×10^{-4} to 1.0×10^{-3}mg/ml ($R^2 \sim 1$) and for carbamazepine from 1.0×10^{-3} to 1.0×10^{-2}mg/ml ($R^2 \sim 1$). The coefficients of variation (CV) for intra- and interassay were all within 4.3%.

The transport rate (dQ/dt) was calculated by plotting the amount of polymer or drug crossing the monolayer versus time (h) and then determining the slope of this relationship. The apparent permeability coefficient (P_{app}, cm s^{-1}) was calculated according to the following equation:

$$P_{app} = \frac{dQ}{dt} * \frac{1}{C_o * A}$$

where dQ/dt is the transport rate (mg/s), C_o is the initial polymer or drug concentration in the donor well (mg/ml), and A is the surface area of the membrane filter in cm^2 [13,32].

2.4.3. Investigation of mmePEG$_{750}$P(CL-co-TMC) transport mechanisms

The effect of biopharmaceutical properties of the polymer-entrapped drugs on their transport across Caco-2 cell monolayers was assessed using two different poorly soluble compounds (chlorothiazide and carbamazepine) which served as model drugs, both solubilized to saturation in 3% (w/v) [^{14}C]-mmePEG$_{750}$P(CL-co-TMC). The apical wells of Caco-2 cell monolayers inserts were filled with the formulations of interest and the basolateral recoveries were analyzed (A to B) for drug and polymer content.

The comparison between the absorption and the excretion of mmePEG$_{750}$P(CL-co-TMC) in Caco-2 cell monolayer was carried out by incubating the polymeric formulations (0.001 and 0.05%; w/v) either at the apical side for the apical to basolateral transport (A to B) or at the basolateral side for the basolateral to apical transport (B to A).

Possible transport via the paracellular route (A to B) was investigated by opening the tight junctions of Caco-2 cells with a 3mM EGTA solution applied 2 times for 30min at 37°C (ethylene glycol-bis(β-aminoethyl ether)-*N*,*N*,*N*',*N*'-tetraacetic acid tetrasodium salt, Sigma, BE) [22]. Apical media were then replaced by EGTA solutions supplemented either with 13μM D-[1-^{14}C]-

Mannitol solution (61.0mCi/mmol) (GE Healthcare Europe GmbH, Diegem, BE) or with [^{14}C]-mmePEG$_{750}$P(CL-co-TMC) formulations (at 0.001, 0.05 or 0.5%; w/v). Basolateral compartments were filled with a 3mM EGTA solution. Negative controls were obtained by performing the experiments in the same conditions but in the absence of EGTA.

Transport of the polymer and the polymer-loaded drug (carbamazepine) was examined on Caco-2 cells and in the FAE model in order to evaluate the influence of M-cells on the transport of polymeric micelles. A carbamazepine solution solubilized to saturation in 0.05% (w/v) mmePEG$_{750}$P(CL-co-TMC) was applied at the apical side of Caco-2 cell monoculture as well as of the FAE co-cultures.

In order to investigate the role of possible endocytosis mechanisms, Caco-2 cell monolayers were incubated (apically and basolaterally) with various endocytosis inhibitors before transport studies. Cells were first preincubated twice with the inhibitor solution for 30min at 37°C, except in the case of azithromycin where a 3h preincubation was required. The inhibitor solutions used in this study were 132μM azithromycin (inhibitor of fluid-phase endocytosis) [33,34], 100μM 5-(*N*-ethyl-*N*-isopropyl)amiloride (EIPA) (inhibitor of macropinocytosis) [22,35], 8μM filipin III (inhibitor of the caveolae pathway) [36,37], 30μM chlorpromazine (inhibitor of receptor-mediated and clathrin-dependent pathway) [38] and 10mM methyl-β-cyclodextrin (MβCD) (inhibitor of the caveolae and clathrin-dependent pathway) [36,39], All materials were commercially obtained from Sigma. Following the preincubation, apical compartments of cell monolayers were loaded with either 0.001% or 0.5% (w/v) of mmePEG$_{750}$P(CL-co-TMC). The inhibitors were present on both sides of the inserts throughout the transport experiment.

Energy-dependent mechanisms were inactivated by two different methods. First, transport was performed at 4°C subsequent to a 15min preincubation at this temperature. Second, the cell ATP content was depleted by exposing cells to a 10mM sodium azide (NaAz)/50mM 2-deoxyglucose (2-DOG) solution [40] (Sigma), before (2 times for 15min) and during the transport experiment (apically and basolaterally) both carried out at 37°C. In both studies, the mmePEG$_{750}$P(CL-co-TMC) (at 0.001 and 0.5%; w/v) formulations were applied apically.

In order to ensure that inhibition of the energy-dependent transport as well as of the investigated endocytosis mechanisms was effective, intracellular uptake of lucifer yellow (Sigma) and dextran tetramethylrhodamine 10,000MW neutral (Invitrogen, Merelbeke, BE), a fluid-phase endocytosis [33,34] and a macropinocytosis tracer [41], respectively, were incubated with cell monolayers under inhibition conditions and their transport was studied (as previously described). Intracellular content of tracers added to the apical side of Caco-2 cell monolayers (1mg/ml) were assayed by fluorimetry using a Perkin-Elmer LS-30 (Beaconsfield, UK) at λ_{exc} 430nm; λ_{em} 540nm for lucifer yellow and at λ_{exc} 555nm; λ_{em} 580nm for dextran tetramethylrhodamine. Briefly, cell monolayers were washed 3 times in cold PBS supplemented with 0.1% (v/v) FBS for 30s and washed 4 times in cold PBS. Cell lysates obtained by incubation in 0.1% (v/v) Triton X-100 (Acros Organics, Geel, BE) were sonicated and their fluorescence was measured [34]. Data were normalized with the intracellular protein content using a Micro BCA™ Protein Assay Reagent Kit (Pierce Biotechnology, Rockford, IL, USA).

2.5. Inhibition of P-gp efflux pumps

The potential inhibitory effect of mmePEG$_{750}$P(CL-co-TMC) on the P-glycoprotein (P-gp) expressed by Caco-2 cells was evaluated by comparing its impact on the transport of indinavir sulphate, a P-gp substrate [42] (generously supplied by MSD Europe INC., Brussels, BE). Cyclosporin A (CyA) (Sigma) [43], a well-known P-gp inhibitor, was used as positive control. The degree of P-gp inhibition was expressed following the equation:

$$\text{Degree of P-gp inhibition} = \left(1 - \frac{[S+I]_{B-A} - [S+I]_{A-B}}{[S]_{B-A} - [S]_{A-B}}\right) * 100$$

where $[S]_{B-A}$ is the P_{app} of the P-gp substrate alone (indinavir) from the basolateral to the apical side and $[S]_{A-B}$ from the apical to basolateral side, $[S+I]_{B-A}$ is the P_{app} of the P-gp substrate in the presence of a potential P-gp inhibitor from the basolateral to the apical side and $[S+I]_{A-B}$ from the apical to basolateral side [44].

The Caco-2 cell monolayers were preincubated at 37°C (2 times for 30min), with either 10μM CyA, mmePEG$_{750}$P(CL-co-TMC) (at 0.001 and 0.05%%; w/v) or HBSS (control). For the A to B transport experiment, a 150μM indinavir solution was applied at the apical side and the basolateral compartments were sampled after 2h incubation at 37°C. The amounts of indinavir were quantified by HPLC-UV according to the method published by Notari et al. [45], which was adapted to our laboratory conditions (see Section 2.4.2). Standard curves for low and high concentrations of indinavir were generated (from 0.5 to 15μM ($R^2 \sim 1$) and from 15 to 300μM ($R^2 \sim 1$), respectively). The coefficients of variation (CV) for intra- and interassay were all within 3.2%.

2.6. Statistical analysis

For all experiments, data are presented as the mean ± SD. Statistical analyses were completed using JMP software (SAS Institute Inc., version 4.0.2). Significance was tested using a one-way ANOVA with a Tukey *post hoc* test for the paracellular, endocytosis and P-gp investigations. Other experiments were tested using a *t*-test. Values of $p < 0.05$ and $p < 0.001$ were considered statistically significant and highly significant, respectively.

3. Results

3.1. Absorption of polymer-solubilized drugs as a function of their biopharmaceutical properties

Carbamazepine and chlorothiazide were selected as model drugs to evaluate the influence of mmePEG$_{750}$P(CL-co-TMC)

on their oral delivery. These materials are representative class II (low solubility — high permeability) and IV (low solubility — low permeability) compounds as described by the Biopharmaceutical Classification System (BCS) [46]. The compounds were solubilized to their saturation solubilities in 3% (w/v) mmePEG$_{750}$P(CL-co-TMC). A 4.4-fold increase in carbamazepine solubility was observed by the use of 3% polymer (0.62 ± 0.0005mg/ml) compared to the carbamazepine solubility in HBSS (0.14 ± 0.001mg/ml). The solubility of chlorothiazide in HBSS (0.26 ± 0.007mg/ml) was moderately improved by its solubilization in 3% polymer (0.36 ± 0.0004mg/ml).

The formulations for the two drugs were applied at the apical side of Caco-2 cell monolayers. In both cases, polymer P_{app}s reached approximately 1.2×10^{-6}cm s^{-1}, whereas the P_{app}s for the entrapped drugs were 1.5×10^{-5} and 5.7×10^{-7}cm s^{-1} for carbamazepine and chlorothiazide, respectively (Fig. 1A). The P_{app}s of drugs in polymer-free formulations were 2.8×10^{-5} and 8.4×10^{-7}cm s^{-1} for carbamazepine and chlorothiazide, respectively. Sampling every 30min of basolateral compartments during the course of the experiment revealed linear passage kinetics ($R^2 > 0.98$) for the polymer as well as for carbamazepine and chlorothiazide (solubilized in 3% mmePEG$_{750}$P(CL-co-TMC) or in water).

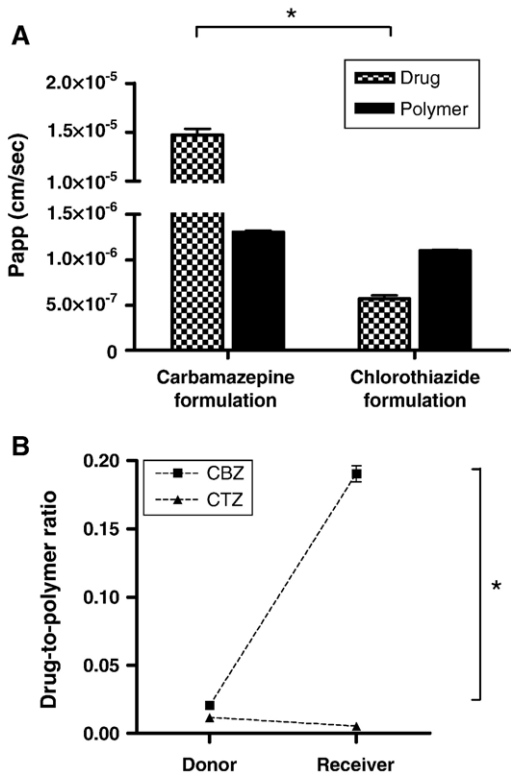

Fig. 1. Apical to basolateral transport across Caco-2 cell monolayers of carbamazepine and chlorothiazide, both solubilized to saturation in 3% w/v mmePEG$_{750}$P(CL-co-TMC) polymer. A. Apparent permeability coefficients (P_{app}) of the carbamazepine formulation (mmePEG$_{750}$P(CL-co-TMC) and carbamazepine) and the chlorothiazide formulation (mmePEG$_{750}$P(CL-co-TMC) and chlorothiazide) in Caco-2 cell monolayers. B. Drug-to-mmePEG$_{750}$P(CL-co-TMC) ratio in donor compartment (apical) at t_0 and in receiver compartment (basolateral) after 120 min of incubation at 37 °C (mean±SD; $n=3$) (*: $p<0.001$).

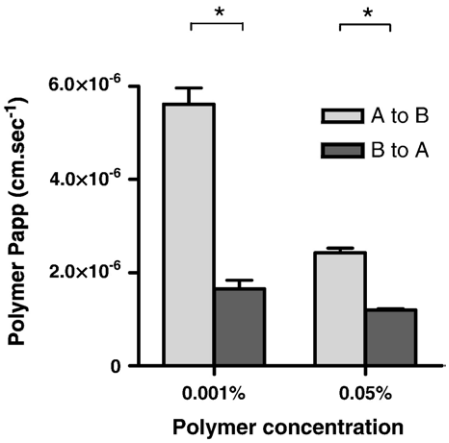

Fig. 2. P_{app}s of mmePEG$_{750}$P(CL-co-TMC) below (0.001%) and above the CMC (0.05%) across Caco-2 cell monolayers from apical to basolateral side (A to B) and *vice versa* (mean±SD; $n=3$) (*: $p<0.001$).

The drug-to-polymer ratios in the donor solutions (at time t_0) for both formulations were in the same range (0.02 and 0.01 w/w) for carbamazepine and chlorothiazide, respectively. After 2h of incubation in Caco-2 cell monolayers, the ratios found in the basolateral compartment for the carbamazepine formulation increased 10 times (0.19), while a 2-fold decrease was observed for chlorothiazide formulation (0.005), as illustrated in Fig. 1B. These results suggest that the polymer and the micelle-loaded drugs cross cell monolayers independently of each other. The reason why the drugs maintain their intrinsic permeability characteristics is likely due to the fact that it is mainly the free drug fraction and not the encapsulated drug which permeates across the cell monolayer.

3.2. Absorption versus excretion of mmePEG$_{750}$P(CL-co-TMC)

The P_{app} related to the polymer absorption (apical to basolateral) was approximately 3 times higher than for its excretion (basolateral to apical) (5.6×10^{-6} and 1.7×10^{-6}cm s^{-1}, respectively) at a polymer concentration just below the CMC (0.001%; w/v) (Fig. 2). Above the CMC (0.05%), the polymer P_{app} was still 2-fold higher in the absorptive direction ($2.4\ 10^{-6}$cm s^{-1}) compared to that in the excretive direction ($1.2\ 10^{-6}$cm s^{-1}). These differences in polymer P_{app}s indicate that the absorption of mmePEG$_{750}$P(CL-co-TMC) results either from an active process or from an enhanced passive transfer.

3.3. Paracellular transport of mmePEG$_{750}$P(CL-co-TMC)

In order to investigate the possible paracellular transport of mmePEG$_{750}$P(CL-co-TMC), its permeation through enterocytes was compared in Caco-2 cell monolayers treated or not treated with a compound designed to open tight junctions. Opening of the tight junctions, induced by EGTA, was associated with a 20-fold increase in mannitol P_{app} (from 3.9×10^{-7} to 7.1×10^{-6}cm s^{-1}), as illustrated in Fig. 3. Mannitol is a well-established paracellular marker. The disruption of tight junctions was also confirmed by measuring cell monolayer

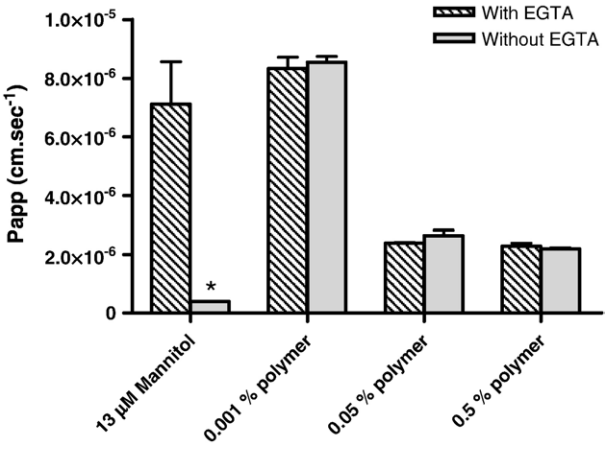

Fig. 3. Apparent permeability coefficients (P_{app}) of mmePEG$_{750}$P(CL-co-TMC) (at 0.001, 0.05 and 0.5%; w/v) and mannitol (13 μM), a paracellular marker, across Caco-2 cell monolayers (from apical to basolateral side) with or without 3 mM EGTA (mean±SD; $n=3$) (*: $p<0.001$ *vs.* mannitol with EGTA).

TEER values, which decreased approximately 20% after 2h of incubation with the EGTA solution compared to the controls. Cells exposed to EGTA-free medium showed no decrement in resistances. The P_{app}s of mmePEG$_{750}$P(CL-co-TMC) were not significantly influenced by the presence of EGTA ($p > 0.05$) over a range of polymer concentrations (0.001, 0.05 or 0.5%; w/v) suggesting that the polymer is transported by routes other than the paracellular route.

3.4. Role of M-cells in the mmePEG$_{750}$P(CL-co-TMC) absorption

To assess whether M-cells play a role in polymeric micelle absorption, the transport rates of carbamazepine solubilized to saturation in 0.05% (w/v) mmePEG$_{750}$P(CL-co-TMC) in Caco-2 cells and in the FAE models were compared (Fig. 4). No significant difference was observed ($p > 0.05$) between the two cell culture models for the P_{app}s of drug as well as for polymers, suggesting that M-cells were not involved in the polymer transfer. The monoclonal Caco-2 cells used in this experiment manifested a slightly different polymer P_{app}s at 0.05% (± 1.5 × 10^{-6}cm s^{-1}) compared to the mean value obtained on ATCC Caco-2 cells employed in the other experiments reported in the present work (± 2.6 × 10^{-6}cm s^{-1}) ($p < 0.001$).

3.5. Active mechanisms involved in the transcytosis of polymeric surfactant

To examine if polymeric micelles are absorbed via active processes, energy-dependent mechanisms and endocytosis were suppressed. Incubating Caco-2 cells at 4°C resulted in a 54% decrease in the mmePEG$_{750}$P(CL-co-TMC) P_{app} when the polymer was applied at 0.001% (w/v) at the apical side, as compared to the control (Fig. 5). This decrease was even more pronounced for a 0.5% polymer concentration where the P_{app} was reduced by 69%. Inhibition of active transport via the depletion of ATP in the cell significantly affected the mmePEG$_{750}$P(CL-co-TMC) transport ($p < 0.001$) when the polymer concentration was above the CMC (0.5%). A 3-fold decrease of cellular ATP (mmol ATP/mg prot) induced a 42% decrease of P_{app} (data not shown).

Other endocytosis inhibitors also influenced mmePEG$_{750}$P(CL-co-TMC) transport across Caco-2 cell monolayers with azithromycin, an inhibitor of fluid-phase endocytosis, being the most potent. The modulator decreased the polymer P_{app} by 34.5% at an applied polymer concentration of 0.5% ($p < 0.001$) without inducing a significant LDH release. Conversely, no effect of azithromycin was observed on the transport of the 0.001% polymer solution. Filipin III and MβCD, both inhibit the caveolae pathway while MβCD also interferes with clathrin-dependent endocytosis, These materials had only a slight impact on the translocation of the polymer below and above its CMC; the first inhibitor increased somewhat the polymer P_{app}s ($p < 0.001$) whereas the second one diminished them moderately ($p < 0.01$). These results are however associated with cellular toxicity based on LDH release from the cytosol wherein filipin III and MβCD induced an LDH leakage of 17.3% and 11.5%, respectively. For monolayers exposed to filipin III and MβCD TEER values dropped to ± 23% of initial values. EIPA (inhibitor of macropinocytosis) and chlorpromazine (inhibitor of the clathrin-dependent and the receptor-mediated endocytosis) did not affect mmePEG$_{750}$P(CL-co-TMC) translocation over the range of polymer concentrations tested. The effectiveness of the inhibitors (azithromycin, AzNa/2-DOG, EIPA and 4°C) was demonstrated using lucifer yellow and dextran tetramethylrhodamine transport as controls and is represented in the inset graphs (A and B) in Fig. 5. Highly significant decreased uptakes were observed for all inhibitions compared to controls ($p < 0.001$).

3.6. Polymer effect on P-gp efflux pumps

In order to evaluate a possible inhibitory effect of mmePEG$_{750}$P(CL-co-TMC) on efflux pumps, which has been reported for other polymeric surfactants [20,21,47], the influence of the polymer on indinavir efflux, a P-gp substrate, was examined. Indinavir sulfate was chosen because of its good aqueous solubility which minimized possible entrapment within the micelle core. The

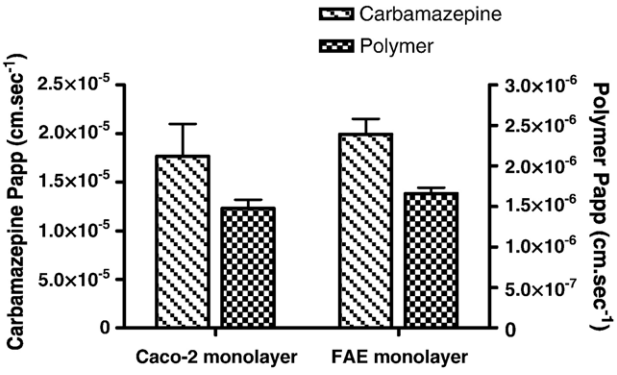

Fig. 4. P_{app}s from apical to basolateral side of polymer-entrapped carbamazepine and mmePEG$_{750}$P(CL-co-TMC) polymer in Caco-2 cell and FAE cell models. Carbamazepine was loaded to saturation in 0.05% mmePEG$_{750}$P(CL-co-TMC) (mean±SD; $n=3$).

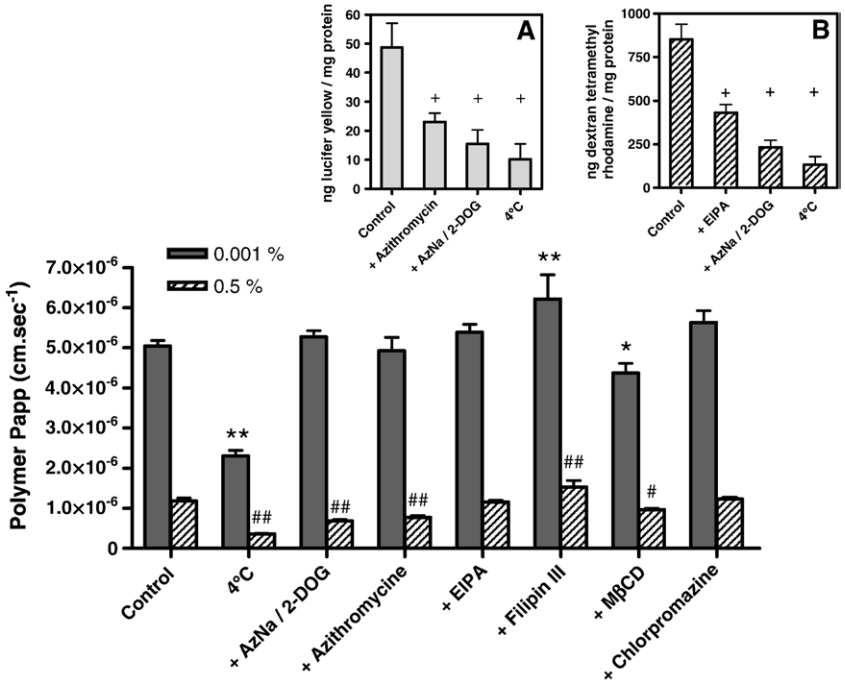

Fig. 5. P_{app}s of mmePEG$_{750}$P(CL-co-TMC) polymer (at 0.001 and 0.5%) across Caco-2 cell monolayers from apical to basolateral side in the presence of inhibitors of energy-dependent mechanisms or endocytosis (mean±SD; $n=5$) ($p<0.01$ (*) and $p<0.001$ (**) *vs.* 0.001% control; $p<0.01$ (#) and $p<0.001$ (##) *vs.* 0.5% control). Inset represents the effect of various endocytosis inhibitors on the intracellular accumulation of endocytic tracers (lucifer yellow for the fluid-phase endocytosis (A) and dextran tetramethylrhodamine 10,000 MW for the macropinocytosis (B)) upon incubation of 1 mg/ml of tracers at the apical pole of Caco-2 cell monolayers (+: $p<0.001$ *vs.* respective control).

indinavir P_{app} values in the absorptive ($\pm 1.50 \times 10^{-6}$cm s^{-1}) and excretive directions ($\pm 3.17 \times 10^{-5}$cm s^{-1}) were not significantly different in the presence or absence of mmePEG$_{750}$P(CL-co-TMC) at 0.001 or at 0.05% (w/v) ($p > 0.05$). These data indicate that P-gp was not inhibited by mmePEG$_{750}$P(CL-co-TMC) while a positive control (10μM cyclosporin A) inhibited P-pg activity by 78% as illustrated in Fig. 6.

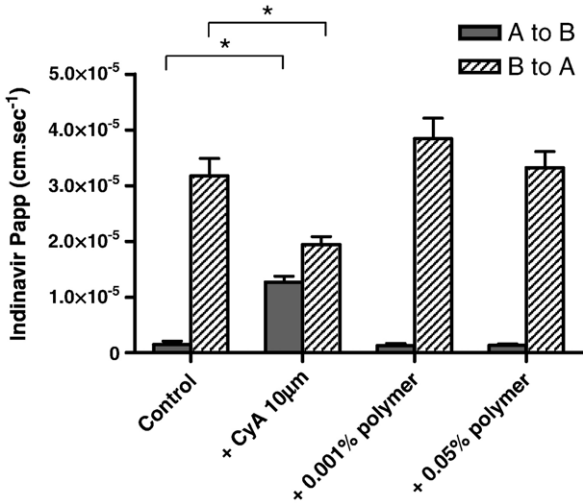

Fig. 6. P_{app}s of indinavir across Caco-2 monolayer from apical to basolateral compartment (A to B) and vice versa (B to A) in the presence of cyclosporin A (CyA) or mmePEG$_{750}$P(CL-co-TMC) (mean±SD; $n=3$) (* = $p<0.001$).

4. Discussion

A polymer which can spontaneously form micelles, namely mmePEG$_{750}$P(CL-co-TMC), has been developed to enhance the apparent solubility of poorly soluble drugs. It has the unexpected capacity of crossing enterocyte-like Caco-2 cell monolayers and to have an oral bioavailability of 40% in rats [15]. Various assessments have revealed that passive diffusion is a viable explanation for how mmePEG$_{750}$P(CL-co-TMC) crosses the intestinal barrier. Previous experiments demonstrated that the mmePEG$_{750}$P(CL-co-TMC) surfactant passively diffused through a PAMPA system without compromising the bilayer integrity [19]. The aim of the current work was therefore to explore energy-and non-energy-dependent processes that could be operating in the transfer of mmePEG$_{750}$P(CL-co-TMC) across enterocytes, as endocytic mechanisms have been invoked to explain this process for other polymeric micelles.

The first part of this work was directed to the study of the paracellular route. In this line of investigation, tight junctions between enterocytes were opened through the use of the Ca^{2+} complexing agent, EGTA. No significant increase of the polymer transport was observed whereas the P_{app} of the mannitol paracellular marker increased approximately 20-fold with TEER values falling at the same time consistent with junctional disruption (Fig. 3). These observations suggested that the paracellular pathway was not involved in the polymer transport. The likely reason being that the paracellular spaces represent less than 1% of the mucosal surface area and that the

pore diameter of the tight junctions does not exceed 10Å whereas mmePEG$_{750}$P(CL-co-TMC) micelles exhibit a hydrodynamic radius of 24nm and unimers have a weight-average molecular weight of ± 5400Da [15,48].

Consequently, the transcellular route was more deeply investigated. Firstly by comparing the absorption of two formulations of 3% mmePEG$_{750}$P(CL-co-TMC) solubilizing either carbamazepine or chlorothiazide to saturation. Data shown in Fig. 1 suggest that micelle-entrapped drugs and polymer crossed Caco-2 cell monolayers independently of each other. In fact, drugs solubilized in mmePEG$_{750}$P(CL-co-TMC) polymeric micelles seemed to maintain their intrinsic permeability characteristics: carbamazepine (BCS class II) permeated more efficiently (± 30 times) the Caco-2 cell monolayer than did chlorothiazide (class IV). These data strongly suggest the passive diffusion of both the free drug fraction and the polymer, more probably as free unimers. This is not surprising if polymeric surface active agents are compared with physiological surfactants like bile salts in that these latter materials are principally absorbed throughout the length of the small intestine by a passive process [49].

Further investigations indicated differences in polymer P_{app}s in the absorptive (apical to basolateral side: A to B) and excretive (B to A) directions through Caco-2 cell monolayers (Fig. 2). Indeed, the absorption rate was up to 3-fold higher than the excretion, suggesting that mmePEG$_{750}$P(CL-co-TMC) polymer undergoes an active A to B transport that probably involves endocytosis. This active transport add up therefore the passive diffusion of mmePEG$_{750}$P(CL-co-TMC) already demonstrated [19]. The likely endocytosis of polymeric micelles was first investigated by evaluating the mmePEG$_{750}$P(CL-co-TMC) P_{app} in an *in vitro* FAE cell model. This model mimics M-cells which are specialized in the uptake of macromolecules and particles via transcytosis [22–24]. Interestingly, no significant differences in the P_{app} of the polymer or the micelle-loaded drug were detected between the Caco-2 cell model and the FAE model (Fig. 4); mmePEG$_{750}$P(CL-co-TMC) micelles being too small (± 24nm) to be efficiently endocytosed by M-cells [50]. Further experiments were then conducted using Caco-2 cell model, which is considered to be a representative model for assessing intestinal uptake of drugs.

In order to examine more thoroughly energy-dependent transport mechanisms, a wide range of inhibitors was applied to the Caco-2 cell monolayers to elucidate the likely mechanism of active transport of mmePEG$_{750}$P(CL-co-TMC) micelles. Results suggested that unimers passively diffused across enterocytes while polymeric micelles utilized fluid-phase pinocytosis for translocation (Fig. 5). Indeed, when ATP was depleted form cells, only P_{app} for polymer concentration above the CMC were affected whereas in case of concentrations below the CMC, no effect was reported. This is consistent with the postulate that only micelles undergo energy-dependent transport and that unimers diffused passively. Interestingly, the use of azithromycin, a specific inhibitor of the clathrin-independent fluid-phase pinocytosis, led to statistically similar results to ATP depletion. A similar decrease in uptake was observed for polymer concentration above the CMC while no effect was reported for transport below the CMC. Fluid-phase pinocytosis is a non-specific process allowing the entry of solutes without binding to the pericellular membrane and showing a proportional rate of uptake over a large range of concentrations [33,34].

Concerning alternative endocytic pathways, the absence of effects induced by chlorpromazine, an inhibitor of receptor-mediated endocytosis, is in agreement with the fact that this process requires specific ligand-receptor recognition that does not take place in the case of mmePEG$_{750}$P(CL-co-TMC) [48]. Likewise, the lack of effect of EIPA on polymer transport is a strong indication that macropinocytosis was not mechanistically relevant. Indeed, this pathway, resulting from membrane ruffling and leading to the formation of large vesicular structure, is a natural feature of phagocytic cells, but rarely applicable to other cell types [51,52]. Finally, depletion of cholesterol from lipid membranes by filipin III or MβCD, which inhibit both the caveolae and the clathrin-dependent endocytosis pathways, had only limited impact on mmePEG$_{750}$P(CL-co-TMC) transport. This might be related to a certain cell permeabilization as illustrated by the TEER value drop and the LDH release.

Interesting information was obtained by incubating cells at 4°C. Indeed, this treatment, which significantly affects energy-dependent processes, did not fully prevent the polymer transfer with at least 30% of the applied mmePEG$_{750}$P(CL-co-TMC) polymer crossing the Caco-2 cell monolayer (Fig. 5). This reinforced the assumption that active transport of mmePEG$_{750}$P (CL-co-TMC) micelles, which may proceed via fluid-phase pinocytosis, is concomitant with passive diffusion of polymeric unimers as illustrated in Fig. 7.

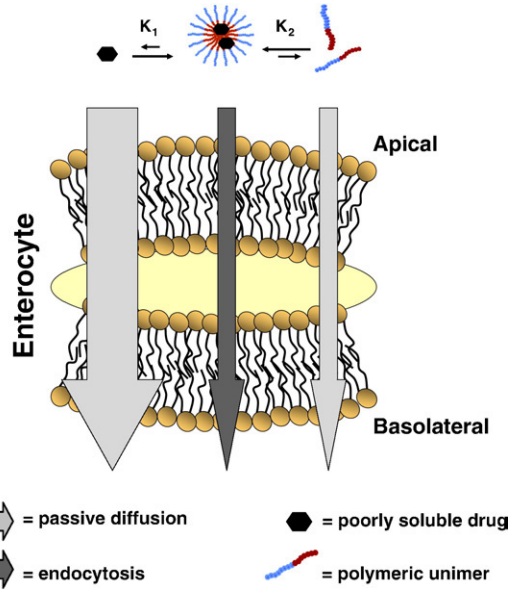

Fig. 7. Schematic representation of the transport pathways for the mmePEG$_{750}$P (CL-co-TMC) polymer, associated micelles and BCS class II drug-laden micelles across enterocytes. The free drug fraction and the unimers passively diffusing whereas drug-loaded micelles undergo a fluid-phase endocytosis. In the case of a BCS class IV drug, the arrow symbolizing the drug permeation should be thinner.

The oral delivery of polymeric micelles, in general, can present a double benefit to sparingly soluble drugs in term of bioavailability by: (i) increasing their apparent solubility and by (ii) slowing intestinal efflux, via P-gp inhibition as in the case of Pluronic P85 [20,21] and MePEG-*b*-PCL [47]). Unfortunately, the mmePEG$_{750}$P(CL-co-TMC) did not appear to inhibit the intestinal P-gp efflux pumps below or above its CMC (Fig. 6). This could be due to the membrane-induced rigification effect of mmePEG$_{750}$P(CL-co-TMC) since in the case of surfactant that inhibit P-gp, membrane fluidization is observed although Zastre et al. [19,47] has recently questioned this theory.

In conclusion, the data collected in this study demonstrate that mmePEG$_{750}$P(CL-co-TMC) and its related unimers and micelles use both passive diffusion and fluid-phase endocytosis in order to cross a Caco-2 model of the intestinal barrier; free unimers diffusing, while micelles follow the endocytic route.

Acknowledgements

The authors express their acknowledgements to F.R.I.A. (Belgian *Fonds pour la Formation à la Recherche dans l'Industrie et dans l'Agriculture*) for a fellowship to Frédéric Mathot as well as the F.R.S.M (Belgian *Fonds de la Recherche Scientifique Médicale*) for support. The authors also wish to thank Cor Janssen (Johnson & Johnson, Beerse, Belgium) for the purity analysis of [^{14}C]-labelled mmePEG$_{750}$P(CL-co-TMC) and Dr. Donatienne Tyteca (ICP, UCL, Brussels, Belgium) for their advice in the endocytosis experiments as well. Additionally, the authors are grateful to CBAT (Somerville, NJ) for the polymer syntheses.

References

[1] A. Lavasanifar, J. Samuel, G. Kwon, Poly(ethylene oxide)-block-poly(L-amino acid) micelles for drug delivery, Adv. Drug Deliv. Rev. 54 (2002) 169–190.
[2] V. Torchilin, Structure and design of polymeric surfactant-based drug delivery systems, J. Control. Release 73 (2001) 137–172.
[3] M-C. Jones, J-C. Leroux, Polymeric micelles — a new generation of colloidal drug carriers, Eur. J. Pharm. Biopharm. 48 (1999) 101–111.
[4] K. Kataoka, A. Harada, Y. Nagasaki, Block copolymer micelles for drug delivery: design, characterization and biological significance, Adv. Drug Deliv. Rev. 47 (2001) 113–131.
[5] G. Kwon, T. Okano, Soluble self-assembled block copolymers for drug delivery, Pharm. Res. 5 (1999) 597–600.
[6] A. Lukyanov, V. Torchilin, Micelles from lipid derivatives of water-soluble polymers as delivery systems for poorly soluble drugs, Adv. Drug Deliv. Rev. 56 (2004) 1273–1289.
[7] G. Kwon, Polymeric micelles for delivery of poorly water-soluble compounds, Crit. Rev. Ther. Drug Carr. Syst. 20 (2003) 357–403.
[8] C. Allen, Y. Yu, A. Eisenberg, D. Maysinger, Cellular internalization of PCL$_{20}$-*b*-PEO$_{44}$ block polymer micelles, BBA-Biomembranes 1421 (1999) 32–38.
[9] J. Liu, F. Zeng, C. Allen, In vivo fate of unimers and micelles of poly (ethylene glycol)-block-poly(caprolactone)copolymer in mice following intravenous administration, Eur. J. Pharm. Biopharm. 65 (2007) 309–319.
[10] M. Francis, M. Cristea, Y. Yang, F. Winnik, Engineering polysaccharide-based polymeric micelles to enhance permeability of cyclosporin A across Caco-2 cells, Pharm. Res. 22 (2005) 209–219.
[11] V. Sant, D. Smith, J-C. Leroux, Enhancement of oral bioavailability of poorly water-soluble drugs by poly(ethylene glycol)-block-poly(alkyl acrylate-co-methacrylic acid) self-assemblies, J. Control. Release 104 (2005) 289–300.
[12] Z. Sezgin, N. Yuksel, T. Baykara, Investigation of pluronic and PEG-PE micelles as carriers of meso-tetraphenyl porphine for oral administration, Int. J. Pharm. 332 (2007) 161–167.
[13] L. Ould-Ouali, M. Noppe, X. Langlois, B. Willems, P. Te Riele, P. Timmerman, M. Brewster, A. Ariën, V. Préat, Self-assembling PEG-p(CL-co-TMC) copolymers for oral delivery of poorly water-soluble drugs: a case study with risperidone, J. Control. Release 102 (3) (2005) 657–668.
[14] L. Ould-Ouali, A. Ariën, J. Rosenblatt, A. Nathan, P. Twaddle, T. Matalenas, M. Borgia, S. Arnold, D. Leroy, M. Dinguizli, L. Rouxhet, M. Brewster, V. Préat, Biodegradable self-assembling PEG-copolymer as vehicle for poorly water-soluble drugs, Pharm. Res. 21 (9) (2004) 1581–1590.
[15] F. Mathot, L. van Beijsterveldt, V. Préat, M. Brewster, A. Ariën, Intestinal uptake and biodistribution of novel self-assembling polymeric micelles after oral administration, J. Control. Release 111 (2006) 47–55.
[16] L. Luo, J. Tam, D. Maysinger, A. Eisenberg, Cellular internalization of poly(ethylene oxide)-*b*-poly(e-caprolactone) diblock copolymer micelles, Bioconjugate Chem. (13) (2002) 1259–1265.
[17] C. Allen, Y. Yisong, A. Eisenberg, D. Maysinger, Cellular internalization of PCL$_{20}$-*b*-PEO$_{44}$ block copolymer micelles, Biochim. Biophys. Acta 1421 (1999) 32–38.
[18] Y.S. Nam, H.S. Kang, J.Y. Park, T.G. Park, S.H. Han, I.S. Chang, New micelle-like polymer aggregates made from PEI-PLGA diblock copolymers: micellar characteristics and cellular uptake, Biomaterials 24 (2003) 2053–2059.
[19] F. Mathot, A. Schanck, F. Van Bambeke, A. Ariën, M. Noppe, M. Brewster, V. Préat, Passive diffusion of polymeric surfactants across lipid bilayers, J. Control. Release 120 (2007) 79–87.
[20] E. Batrakova, S. Li, S. Vinogradov, V. Alakhov, D. Miller, A. Kabanov, Mechanism of pluronic effect on P-glycoprotein efflux system in blood-brain barrier: contributions of energy depletion and membrane fluidization, J. Pharmacol. Exp. Ther. 299 (2001) 483–493.
[21] E. Batrakova, S. Li, V. Alakhov, A. Kabanov, Effect of pluronic P85 on ATPase activity of drug efflux transporters, Pharm. Res. 21 (2004) 2226–2233.
[22] A. des Rieux, V. Fievez, I. Théate, J. Mast, V. Préat, Y-J. Schneider, An improved in vitro model of human intestinal follicle-associated epithelium to study nanoparticle transport by M cells, Eur. J. Pharm. Sci. 5 (2007) 380–391.
[23] A. des Rieux, V. Fievez, M. Momtaz, C. Detrembleur, M. Alonso-Sande, J. Van Gelder, A. Cauvin, Y-J. Schneider, V. Préat, Helodermine-loaded nanoparticles: characterization and transport across an in vitro model of the follicle-associated epithelium, J. Control. Release 118 (2007) 294–302.
[24] A. Honbo, Y. Masaoka, M. Kataoka, S. Sakuma, E. Ragnarsson, P. Artursson, S. Yamashita, Development of an in vitro M-cell model for macromolecule transport, Proceedings of the 19th Annual Meeting of JSSX, 2004.
[25] R. Bezwada, S. Arnold, S. Shalaby, B. Williams, Liquid absorbable polymers for parenteral applications, U.S. Patent 5, 653 992 (A) (1997).
[26] M. Mizutani, S. Arnold, S. Shalaby, Liquid phenylazide-end-capped polymers of caprolactone and trimethylene carbonate: preparation, photocuring characteristics and surface layering, Biomacromolecules 3 (2002) 668–675.
[27] J. Dressman, D. Fleisher, G. Amidon, Physicochemical model for dose-dependent drug absorption, J. Pharm. Sci. 73 (1984) 1274–1279.
[28] A. Arena, J. Philips, Drug transport assays in a 96-well system: reproducibility and correlation to human absorption, Application note, Millipore, http://www.millipore.com/publications.nsf/docs/ps2745en00.
[29] A. Owen, M. Pirmohamed, J. Tettey, P. Morgan, D. Chadwick, K. Park, Carbamazepine is not a substrate for P-glycoprotein, Br. J. Clin. Pharmacol. 51 (2001) 345–349.
[30] V. Ulvi, H. Keski-Hynnilä, First-derivative UV spectrophotometric and high-performance liquid chromatographic analysis of some thiazide diuretics in the presence of their photodecomposition products, J. Pharm. Biomed. Anal. 12 (1994) 917–922.
[31] D. Chollet, E. Castella, P. Combe, V. Arnera, High-speed liquid chromatographic method for the monitoring of carbamazepine and its

active metabolite, carbamazepine-10,11-epoxide, in human plasma, J. Chromatogr., B 683 (1996) 237–243.
[32] P. Artursson, J. Karlsson, Correlation between oral drug absorption in humans and apparent drug permeability coefficients in human intestinal epithelial (Caco-2) cells, Biochem. Biophys. Res. Commun. 175 (1991) 880–885.
[33] D. Tyteca, P. van Der Smissen, F. van Bambeke, K. Leys, P. Tulkens, P. Courtoy, M-P. Mingeot-Leclercq, Azithromycin, a lysosomotropic antibiotic, impairs fluid-phase pinocytosis in cultured fibroblasts, Eur. J. Cell Biol. 80 (2001) 466–478.
[34] D. Tyteca, P. Van der Smissen, M. Mettlen, F. Van Bambeke, P. Tulkens, M-P. Mingeot-Leclercq, P. Courtoy, Azithromycin, a lysosomotropic antibiotic, has distinct effects on fluid-phase and receptor-mediated endocytosis, but does not impair phagocytosis in J774 macrophages, Exp. Cell Res. 281 (2002) 86–100.
[35] E. Ragnarsson, Effects of microparticles drug delivery systems: tissue responses and transcellular transport, Thesis (2006), http://publications.uu.se/theses/abstract.xsql?dbid=6260.
[36] M. Torgersen, G. Skretting, B. van Deurs, K. Sandvig, Internalization of cholera toxin by different endocytic mechanisms, J. Cell Sci. 114 (2001) 3737–3747.
[37] P. Orlandi, P. Fishman, Filipin-dependent inhibition of cholera toxin: evidence for toxin internalization and activation through caveolae-like domains, J. Cell Biol. 141 (1998) 905–915.
[38] T. Gilbert, A. Le Bivic, A. Quaroni, E. Rodriguez-Boulan, Microtubular organization and its involvement in the biogenetic pathways of plasma membrane proteins in Caco-2 intestinal epithelial cells, J. Cell Biol. 113 (1991) 275–288.
[39] S. Rodal, G. Skretting, O. Garred, F. Vilhardt, B. van Deurs, K. Sandvig, Extraction of cholesterol with methyl-b-cyclodextrin perturbs formation of clhathrin-coated endocytic vesicles, Mol. Biol. Cell 10 (1999) 961–974.
[40] S. Lowes, N. Simmons, Multiple pathways for fluoroquinolone secretion by human intestinal epithelial (Caco-2) cells, Br. J. Pharmacol. 135 (2002) 1263–1275.
[41] A. Ivanov, A. Nusrat, C. Parkos, Endocytosis of epithelial apical junctional proteins by a clathrin-mediated pathway into a unique storage compartment, Mol. Biol. Cell 15 (2004) 176–188.
[42] J. Hochman, M. Chiba, J. Nishime, M. Yamazaki, J. Lin, Influence of P-glycoprotein on the transport and the metabolism of indinavir in Caco-2 cells expressing cytochrome P-450 3A4, J. Pharmacol. Exp. Ther. 292 (2000) 310–318.
[43] A. Braun, S. Hammerle, K. Suda, B. Rothen-Rutishauser, M. Gunthert, S. Kramer, H. Wunderli-Allenspach, Cell cultures as tools in biopharmacy, review, Eur. J. Pharm. Sci. 11 (2000) S51–S60.
[44] R. Kim, C. Wendel, B. Leake, M. Fromm, P. Dempsey, M. Roden, F. Belas, A. Chaudhary, D. Roden, A. Wood, G. Wilkinson, Interrelationship between substrates and inhibitors of human CYP3A and P-gp, Pharm. Res. 16 (1999) 408–414.
[45] S. Notari, A. Bocedi, G. Ippolito, P. Narciso, L. Pucillo, G. Tossini, R. Donnorso, F. Gasparrini, P. Ascenzi, Simultaneous determination of 16 anti-HIV drugs in human plasma by high-performance liquid chromatography, J. Chromatogr., B 831 (2006) 258–266.
[46] G. Amidon, H. Lennernas, V. Shah, J. Crison, A theoretical basis for a biopharmaceutic drug classification: the correlation of in vitro drug product dissolution and in vivo bioavailability, Pharm. Res. 12 (1995) 413–420.
[47] J. Zastre, J. Jackson, W. Wong, H. Burt, Methoxypolyethylene glycol-block-polycaprolactone diblock copolymers reduce P-glycoprotein efflux in the absence of membrane fluidization effect while stimulating P-glycoprotein ATPase activity, J. Pharm. Sci. 96 (2007) 864–875.
[48] T. Jung, W. Kamm, A. Breitenbach, E. Kaiserling, J.X. Xiao, T. Kissel, Biodegradable nanoparticles for oral delivery of peptides: is there a role for polymers to affect mucosal uptake? Review, Eur. J. Pharm. Biopharm. 50 (2000) 147–160.
[49] P. Swaan, F. Szoka, S. Øie, Use of the intestinal and hepatic bile acid transporters for drug delivery, Adv. Drug Deliv. Rev. 20 (1996) 59–82.
[50] E. Gullberg, Particle transcytosis across the human intestinal epithelium: model development and target identification for improved drug delivery, Thesis (2005).
[51] L. Johannes, C. Lamaze, Clathrin-dependent or not: is it still the question? Review, Traffic 3 (2002) 443–451.
[52] D. Tyteca, Azithromycin, a pharmacological agent with selectively impairs some pathways of endocytosis: characterization, interests and mechanism of action, Thesis (2001).